Journal of Applied Analysis and Computation
Volume 12, Number 3, June 2022, 1007–1021
Website:http://www.jaac-online.com
DOI:10.11948/20220098

A NEW APPROACH TO DATA ASSIMILATION FOR NUMERICAL WEATHER FORECASTING AND CLIMATE PREDICTION*

Wansuo Duan[1,2], Rong Feng[1], Lichao Yang[1,†] and Lin Jiang[1,2]

Dedicated to Professor Jibin Li on the occasion of his 80th birthday.

Abstract Based on the review of nonlinear forcing singular vector (NFSV) for dealing with the most disturbing model error and the optimal forcing vector (OFV) for neutralizing model error effect, the NFSV-data assimilation (NFSV-DA) approach was reinterpreted as neutralizing combined effect of model errors and initial errors in predictions. Then the calculation of adjoint-related gradient was derived for solving the NFSV-DA. With the applications to El Niño and tropical cyclone predictabilities, the usefulness of the NFSV-DA was emphasized for improving prediction skill of weather and climate. Furthermore, how to further consummate the NFSV-DA was discussed and future works were prospected. It is finally expected that the NFSV-DA becomes operational and greatly increases the prediction level of weather and climate.

Keywords Data assimilation, optimization problem, prediction error, predictability.

MSC(2010) 86A08, 86A10.

1. Introduction

The essence of numerical weather forecast and climate prediction is to solve an initial value problem of complex partial differential equations. Due to the lack of observations, errors often occur in initial values and then greatly limit forecasting levels of weather and climate [26,28]. Field observations are never dense enough to satisfy the demands of initialization in predictions; furthermore, it is very costly to acquire these observations. Therefore, increasing additional observations in a few key areas but not over the full field (i.e., target observations; [30]) and assimilating them to initial field have been thought of as an economic and effective way to reduce the effects of initial errors [24,26]. Besides, current numerical models cannot yet exactly describe the motions of atmosphere and ocean fluids and there exist inevitable model errors, which also severely influence the accuracy of prediction results [12,23]. That is to say, it is both initial errors and model errors that jointly

†The corresponding author. Email: yanglc@mail.iap.ac.cn(L. Yang)
1LASG, Institute of Atmospheric Physics, Chinese Academy of Sciences, Beijing 100029, China
2University of Chinese Academy of Sciences, Beijing 100029, China
*This work was jointly sponsored by the National Nature Scientific Foundation of China (Nos. 41525017, 41930971).

lead to prediction errors of weather and climate. The current facts, as discussed above, are the lack of adequate observations and the imperfect of numerical models; then significant initial errors and model errors are still non-negligible in current predictions of weather and climate. Even so, the meteorologists have to conduct operational forecasts to serve the demand of disaster prevention and mitigation. In this situation, one has to encounter such a challenging question as how to maximize the forecasting capability of a prediction system by considering both the initial errors and model errors. To address this question, two aspects of studies should be concerned. One is to explore the reasons of yielding prediction uncertainties; and the other is to study the methods to reduce prediction uncertainties [27].

This paper mainly focuses on the discussion of the second aspect of studies, that is, the methods to reduce prediction uncertainties. Generally, a present complete prediction strategy is as follows. After identifying the major error source of prediction uncertainties, an advanced assimilation method is applied to optimize initial field by using the most useful observations (for example, “target observations”). With the optimized initial field, numerical model is integrated and a deterministic prediction is made. Keep this prediction in mind, multiply initial perturbations are yielded to disturb this prediction and conduct ensemble forecasting, which cannot only give a deterministic prediction by adopting ensemble mean but also estimate its prediction uncertainties by evaluating ensemble spread, eventually obtaining a complete high-quality prediction product. From this strategy, it is easily recognized that data assimilation is essential for achieving a complete high-quality prediction product.

Bauer et al. [3] have stated that a quiet revolution occurred in the past three decades and numerical weather forecasting level improved almost 30%, especially in the Southern Hemisphere. One of the major causes of this great improvement is thought of as the use of variational data assimilation and satellite data since the late 1990s. It is obvious that data assimilation plays a key role in current weather forecast and climate prediction. However, the classical data assimilation is established on the assumption of perfect model and only consists of reducing the effects of initial errors [18]. Model errors, as mentioned above, is another source of prediction errors; especially, more and more studies began to explore its roles in yielding prediction uncertainties for achieving more accurate predictions. For example, Wang et al. [34] demonstrated that the major cause of the low skill of weather ensemble forecasting is the effect of model systematic errors; the Intergovernmental Panel on Climate Change Fifth Assessment Report (IPCC AR5) also considered the effects of model errors and its interaction with initial errors when redefining the climate predictability [19]. In view of this situation, it is urgently important to reduce effects of model errors and their interactions with initial errors and finally improve prediction level of weather and climate. Then, a tough question arises: how can one achieve such a goal?

For the approaches to reduce model error effects, the one flashing into our mind is to improve numerical models by updating and/or improving physical parameterization schemes or to enhance their spatial-temporal resolutions. However, model error sources are of diversity and complexity; furthermore, they are interactive, and then the phenomenon of pressing gourd dipper float often happens when debugging numerical models. It is therefore impossible to identify every model error source and debug them to reduce their effects on prediction results. Then whether or not one can consider combined effect of kinds of model error sources from a macroscopic perspective instead of the micro details of each model error source? furthermore, in view of the fact that data assimilation has been successfully used to reduce initial error effects and played a key role in improving prediction skill of weather and climate, it is wonder if data assimilation is also feasible for decreasing combined effect of model errors.

To address these questions, the key issue to be first explored is how to describe the combined effect of kinds of model error sources. Duan and Zhou [12] proposed a nonlinear forcing singular vector (NFSV) approach to reveal the model error that causes the largest prediction error (also see [11]). They proposed to adopt a tendency perturbation for depicting combined effect of kinds of model error sources. Inspired by the NFSV, Duan et al. [9] further introduced an optimal forcing vector (OFV) approach, in attempt to obtaining an appropriate tendency correction term to offset combined effect of model errors by assimilating relevant observations (also see [7]). Then in the present article, we will synthetically review the NFSV for dealing with optimally-growing model errors and the OFV for offsetting model error effects and update the OFV as a new data assimilation approach for dealing with combined effect of model errors and its interaction with initial errors, finally reviewing its usefulness in weather and climate predictability and future possible uses toward operational predictions of weather and climate.

The remainder of the paper is organized as follows. The NFSV-data assimilation (NFSV-DA) approach is formulated in section 2 and its calculation is derived in section 3. Section 4 gives a review on the usefulness of the NFSV-DA in the predictability studies of El Niño and tropical cyclone. Finally, section 5 provides a summary and a discussion to the further work and possible uses of the NFSV-DA.

2. The NFSV-DA for neutralizing combined effect of model errors and its interaction with initial errors

To reveal spatial dependence of combined effect of kinds of model errors, Duan and Zhou [12] used a tendency perturbation to describe combined effect of model errors and proposed the NFSV method to disclose the model error of particular structure that is responsible for the largest deviation from the reference state. Obviously, the NFSV is related to a maximization problem. A dynamical equation for a state vector $\boldsymbol{U}$ is written as in the Eq.(2.1),

$$\begin{cases} \frac{\partial \boldsymbol{U}}{\partial t} = F(\boldsymbol{U}(\boldsymbol{x},t)), \\ \boldsymbol{U}\,|_{t=0} = \boldsymbol{U}_0, \qquad\qquad \text{in} \quad \Omega \times [0,\tau] \end{cases} \tag{2.1}$$

where $\boldsymbol{U}(\boldsymbol{x},t)$=$(\boldsymbol{U}_1(\boldsymbol{x},t), \boldsymbol{U}_2(\boldsymbol{x},t), \cdots, \boldsymbol{U}_n(\boldsymbol{x},t))$ and $\boldsymbol{U}_0$ is its initial state; $(\boldsymbol{x},t) \in \Omega \times [0,\tau]$ with Ω being a domain in R^n and t being the time of $\tau < +\infty$; and F is a nonlinear operator. If the Eq.(2.1) and $\boldsymbol{U}_0$ are exactly known, the final state at the future time τ can be solved by integrating the Eq.(2.1). Such final state $\boldsymbol{U}(\boldsymbol{x},\tau)$ can be expressed as in Eq.(2.2)

$$\boldsymbol{U}(\boldsymbol{x},\tau) = M_\tau(\boldsymbol{U}_0), \tag{2.2}$$

where M_τ is the propagator of the Eq.(2.1), which "propagates" the initial state $\boldsymbol{U}_0$ to the final time τ and output the final state $\boldsymbol{U}(\boldsymbol{x},\tau)$. In numerical weather forecast and climate prediction, a prediction is usually contaminated by both initial errors and model errors. With a tendency perturbation $\boldsymbol{f}(\boldsymbol{x},t)$ describing combined effect of model errors, a realistic prediction model can be of the equations as in Eq.(2.3).

$$\begin{cases} \frac{\partial(\boldsymbol{U}+\boldsymbol{u})}{\partial t} = F(\boldsymbol{U}+\boldsymbol{u}) + \boldsymbol{f}(\boldsymbol{x},t), \\ \boldsymbol{U}+\boldsymbol{u}\mid_{t=0} = \boldsymbol{U}_0 + \boldsymbol{u}_0, \end{cases} \tag{2.3}$$

where $\boldsymbol{u}_0$ is initial error, then $\boldsymbol{u}$ represents prediction error caused by both initial error and model error. If $M_\tau(\boldsymbol{f})$ denotes the propagator of the Eq.(2.3), the final state can be expressed as in the Eq.(2.4).

$$M_\tau(\boldsymbol{f})(\boldsymbol{U}_0+\boldsymbol{u}_0) = \boldsymbol{U}(\boldsymbol{x},\tau) + \boldsymbol{u}(\boldsymbol{x},\tau), \tag{2.4}$$

where $\boldsymbol{U}(\boldsymbol{x},\tau) = M_\tau(0)(\boldsymbol{U}_0) = M_\tau(\boldsymbol{U}_0)$ [see Eq.(2.2)]. With the assumption of perfect initial field and constant tendency perturbation $\boldsymbol{f}(\boldsymbol{x})$ for simplicity, the NFSV can be defined as follows.

$$J_\delta(\boldsymbol{f}_\delta) = \max_{\|\boldsymbol{f}\|\le\delta} J(\boldsymbol{f}), \tag{2.5}$$

where

$$J(\boldsymbol{f}) = \|M_\tau(\boldsymbol{f})(\boldsymbol{U}_0) - M_\tau(0)(\boldsymbol{U}_0)\| \tag{2.6}$$

and $\|\boldsymbol{f}\|\le\delta$ is the constraint condition defined by the L2 norm $\|\cdot\|$ and constrains the maximum amplitude of $\boldsymbol{f}(x)$ (i.e. combined effect of model errors). The cost function J evaluates the amplitude of the prediction error with respect to the reference state $M_\tau(0)(\boldsymbol{U}_0)$ caused by $\boldsymbol{f}$. After solving the Eq.(2.5), one can obtain the NFSV $\boldsymbol{f}_\delta$. The NFSV represents the model error that causes the largest prediction error and has particular spatial structure responsible for its optimal growth.

Along the thinking of the tendency perturbation describing the combined effect of model errors, Duan et al. [9] further suggested an optimal forcing vector (OFV) approach to obtain an appropriate correction term for minimizing the distance between model simulations and observations when only considering effect of model errors. In this paper, it will be further updated to reveal the correction term that makes the model simulation with initial error and model error effects closest to the observation at the final time τ. Then the renewed OFV can be expressed as the following minimization problem.

$$J_o(f'_o) = \min_{f'} \|M_\tau(f)(f')(U_0+u_0) - U^{obs}(x,\tau)\|, \tag{2.7}$$

where $U^{obs}(x,\tau)$ is the observation at time τ, $M_\tau(f)$ is the forecast model with model errors and the model error f here needs to be offset by the tendency perturbation f' to be solved, and $M_\tau(f)(U_0+u_0)$ represents reference simulation contaminated by initial error and model error. Then the Eq.(2.7) solves the renewed OFV f'_o.

Relating the renewed OFV to NFSV, if concerned problem is applied to the prediction model Eq.(2.3), the NFSV can be understood as the tendency perturbation f' that is superimposed on f and of most sensitivities to the reference simulation $M_\tau(f)(U_0+u_0)$ and this reference simulation can thus be greatly improved after filtering model errors suggested by the NFSV sensitivity; then in this situation for the renewed OFV, it can be interpreted as the tendency perturbation f' that makes the updated simulation $M_\tau(f)(f')(U_0+u_0)$ to have the largest departure from the reference simulation $M_\tau(f)(U_0+u_0)$ but has the constraint to make the updated simulation is closest to the observation. In this way, the renewed OFV can also be expressed by the Eq.(2.8) as a maximization problem with the constraint $f' \in \Omega$, which is similar to that for the NFSV mathematically.

$$J(f'_o) = \max_{f' \in \Omega} \| M_\tau(f)(f')(U_0 + u_0) - M_\tau(f)(U_0 + u_0) \|, \tag{2.8}$$

where

$$\Omega = \{ f' | J(f') = \min_{f'} \| M_\tau(f)(f')(U_0 + u_0) - U^{obs}(x, \tau) \| \}.$$

The OFV and NFSV are essentially different in dynamics; and the former is related to a minimization problem for searching for tendency perturbation to minimize the distance between simulation and observation while the latter is a maximization problem for looking for the most sensitive tendency perturbation that maximizes the departure from the reference simulation. Nevertheless, in this paper they are mathematically unified into a NFSV-related maximization problem (Eq. (2.8)); furthermore, they are mutually supported dynamically. Therefore, to emphasize the unity of NFSV and OFV in mathematics and simultaneously reflect the difference of them in dynamics, the renewed OFV is restated as "NFSV-DA"[also see Tao and Duan [31]].

From the definition of the NFSV-DA, it is easily seen that the correction term determined by the NFSV-DA is applicable for state simulations that have had relevant observations for reference. In fact, the NFSV-DA with initial error effects being neglected, i.e. the original OFV, had been applied to correct the simulation of ENSO events and then constructed the optimal observation array for improving initialization of ENSO predictions [7]. Also, with the application of an ENSO model corrected by the NFSV-DA, the role of nonlinear physical processes in the formulation of the ENSO modes was clearly evaluated, thus providing a new interpretation to the ENSO diversities [6]. However, when we are operating a realistic prediction, there are not referable observations during the prediction period and, thus, we cannot obtain the correction term of the NFSV-DA timely. In view of this limitation, Tao and Duan [31] established a statistical model to depict the lead-lag relationship between the correction term determined by the NFSV-DA and the observed sea surface temperature anomaly using historical data for El Niño-Southern Oscillation (ENSO) prediction. Clearly, Tao and Duan [31] suggested a way to determine the correction term during prediction period. Then when the prediction starts, the statistical model would tell us what correction term should be used in the prediction period; that is to say, which correction term one should adopt to offset the future prediction error caused by combined effect of model errors and initial errors. As such, the NFSV-DA has the potential for applications to real-time prediction of weather and climate.

The Eqs. (2.7) and (2.8) for NFSV-DA ensure the smallest distance between the predictions and the observations. In fact, one can also define the NFSV-DA to make the prediction results during the whole prediction period closest to the observations. That is, it solves the following assimilation problem.

$$J_o(f'_o) = \min_{f'} \sum_{t=0}^{\tau} \| M_t(f)(f')(U_0 + u_0) - U^{obs}(x, t) \| \tag{2.9}$$

where $t \in [0, \tau]$ is the time during the prediction period from 0 to time τ.

As discussed above, the renewed OFV is granted with a new interpretation according to the combined effect of model errors and initial errors and the NFSV-DA is formed for simulations of weather and climate. Then it becomes an approach to correct combined effect of model errors and initial errors associated with numerical weather forecast and climate prediction by considering the relationship between the correction term and the observations at the start time of predictions, thus providing a new idea for improving prediction level of weather and climate (also see [32]).

3. The calculation of NFSV-DA

The NFSV-DA defined by both Eq.(2.7) and Eq.(2.9) are respectively related to an unconstrained optimization problem. For the sake of simplicity, we directly use M_t instead of $M_t(f)$ above and then the basic problem they solve is the minimal value of the Eq.(3.1).

$$J(f') = \frac{1}{2}\|M_t(f')(U_0 + u_0) - U^{obs}(x,t)\|^2 \tag{3.1}$$

To solve the minimal value of Eq.(3.1), the gradient of the cost function J with respect to f' is required, which represents the fastest-descending direction of J toward its minimal value. In numerical weather forecast and climate prediction, the minimization problem of the Eq.(3.1) is often relevant with high dimensions of numerical models. For such large-scale optimization, the gradient is usually calculated efficiently by integrating the adjoint of numerical models. To facilitate readers, we derive it here based on the NFSV in Duan and Zhou [12] and Feng and Duan [14]. If the Eq.(3.1) adopts the L2 norm, it can be rewritten as an inner product form with the sign $< \cdot >$.

$$J(f') = \frac{1}{2} < \boldsymbol{u}(t), \boldsymbol{u}(t) >, \tag{3.2}$$

where $\boldsymbol{u}(t) = M_t(\boldsymbol{f}')(\boldsymbol{U}_0 + \boldsymbol{u}_0) - U^{obs}(x,t)$

The first-order variation of J follows.

$$\delta J =< \boldsymbol{u}(t), \delta \boldsymbol{u}(t) >=< \frac{\partial J}{\partial \boldsymbol{u}_0}, \delta \boldsymbol{u}_0 > + < \frac{\partial J}{\partial f'}, \delta \boldsymbol{f}' >, \tag{3.3}$$

where $\delta \boldsymbol{u}(t)$ and $\delta \boldsymbol{f}'$ are the solutions of the following tangent linear model.

$$\begin{cases} \frac{\partial \delta \boldsymbol{u}}{\partial t} = \frac{\partial F(\boldsymbol{U}(t) + \boldsymbol{u}(t))}{\partial \boldsymbol{u}} \delta \boldsymbol{u} + \delta \boldsymbol{f}', \\ \frac{\partial \delta \boldsymbol{f}'}{\partial t} = 0, \\ \delta \boldsymbol{u}|_{t=0} = \delta \boldsymbol{u}_0, \\ \delta \boldsymbol{f}'|_{t=0} = \delta \boldsymbol{f}'. \end{cases} \tag{3.4}$$

Two Lagrangian Multipliers λ_1 and λ_2 are introduced and there obtain that

$$\begin{aligned} \delta J = &< \boldsymbol{u}(t), \delta \boldsymbol{u}(t) > - \int_0^t < \lambda_1(t'), \frac{\partial \delta \boldsymbol{u}}{\partial t'} - \frac{\partial F(\boldsymbol{U}(t') + \boldsymbol{u}(t'))}{\partial \boldsymbol{u}} \delta \boldsymbol{u} - \delta \boldsymbol{f}' > dt' \\ &- \int_0^t < \lambda_2(t'), \frac{\partial \delta \boldsymbol{f}'}{\partial t'} > dt'. \end{aligned} \tag{3.5}$$

An integration by parts is applied to the Eq.(3.5), then one can get

$$\int_0^t < \lambda_1(t'), \frac{\partial \delta \boldsymbol{u}}{\partial t'} > dt' = \int_0^t \frac{\partial}{\partial t'} < \lambda_1(t'), \delta \boldsymbol{u} > dt' - \int_0^t < \frac{\partial \lambda_1(t')}{\partial t'}, \delta \boldsymbol{u} > dt'$$
$$= < \lambda_1(t), \delta \boldsymbol{u}(t) > - < \lambda_1(0), \delta \boldsymbol{u}(0) > - \int_0^t < \frac{\partial \lambda_1(t')}{\partial t'}, \delta \boldsymbol{u} > dt'$$

and

$$\begin{aligned}
&\int_0^t < \lambda_2(t'), \frac{\partial \delta \boldsymbol{f}'}{\partial t'} > dt' \\
&= \int_0^t \frac{\partial}{\partial t'} < \lambda_2(t'), \delta \boldsymbol{f}' > dt' - \int_0^t < \frac{\partial \lambda_2(t')}{\partial t'}, \delta \boldsymbol{f}' > dt' \\
&= < \lambda_2(t), \delta \boldsymbol{f}'(t) > - < \lambda_2(0), \delta \boldsymbol{f}'(0) > - \int_0^t < \frac{\partial \lambda_2(t')}{\partial t'}, \delta \boldsymbol{f}' > dt' \\
&= < \lambda_2(t), \delta \boldsymbol{f}' > - < \lambda_2(0), \delta \boldsymbol{f}' > - \int_0^t < \frac{\partial \lambda_2(t')}{\partial t'}, \delta \boldsymbol{f}' > dt'.
\end{aligned}$$

Then δJ is derived as follows.

$$\begin{aligned}
\delta J = &\int_0^t < \frac{\partial \lambda_1(t')}{\partial t}, \delta \mathbf{u} > dt' + < \boldsymbol{u}(t) - \lambda_1(t), \delta \boldsymbol{u}(t) > + < \lambda_1(0), \delta \boldsymbol{u}(0) > \\
&+ \int_0^t < \lambda_1(t'), \left[\frac{\partial F(\boldsymbol{U} + \boldsymbol{u})}{\partial \boldsymbol{u}} \right] \delta \boldsymbol{u} > dt' + \int_0^t < \lambda_1(t'), \delta \boldsymbol{f}' > dt' \\
&+ \int_0^t < \frac{\partial \lambda_2(t')}{\partial t}, \delta \boldsymbol{f}' > dt' + < \lambda_2(0), \delta \boldsymbol{f}' > - < \lambda_2(t), \delta \boldsymbol{f}' > \\
= &\int_0^t < \frac{\partial \lambda_1(t')}{\partial t}, \delta \boldsymbol{u} > dt' + < \boldsymbol{u}(t) - \lambda_1(t), \delta \boldsymbol{u}(t) > + < \lambda_1(0), \delta \boldsymbol{u}(0) > \\
&+ \int_0^t < \left[\frac{\partial F(\boldsymbol{U} + \boldsymbol{u})}{\partial \boldsymbol{u}} \right]^* \lambda_1(t'), \delta \boldsymbol{u} > dt' + \int_0^t < \lambda_1(t'), \delta \boldsymbol{f}' > dt' \\
&+ \int_0^t < \frac{\partial \lambda_2(t')}{\partial t}, \delta \boldsymbol{f}' > dt' + < \lambda_2(0), \delta \boldsymbol{f}' > + < 0 - \lambda_2(t), \delta \boldsymbol{f}' >,
\end{aligned} \tag{3.6}$$

where $[\cdot]^*$ denotes an adjoint. Comparison is performed between Eqs.(3.6) and (3.3) and the gradients of J with respect to initial perturbations $\boldsymbol{u}_0$ (see Eq.(3.7)) and tendency perturbations $\boldsymbol{f}'$ (see Eq.(3.8)) can be obtained, respectively.

$$\frac{\partial J}{\partial \boldsymbol{u}_0} = -\lambda_1(0), \tag{3.7}$$

and

$$\frac{\partial J}{\partial \boldsymbol{f}'} = -\lambda_2(0), \tag{3.8}$$

where $\lambda_1(t)$ and $\lambda_2(t)$ satisfies

$$\begin{cases} \frac{\partial \lambda_1(t')}{\partial t'} + \left[\frac{\partial F(\boldsymbol{U}+\boldsymbol{u})}{\partial \boldsymbol{u}}\right]^* \lambda_1(t') = 0, \\ \frac{\partial \lambda_2(t')}{\partial t'} + \lambda_1(t') = 0, \\ \lambda_1|_{t'=0} = \boldsymbol{u}(t), \\ \lambda_2|_{t'=t} = 0, \end{cases} \tag{3.9}$$

and the Eq.(3.9) is the adjoint equation of tangent linear model Eq.(3.4).

It is clear that the gradient associated with the NFSV-DA can be calculated with $\frac{\partial J}{\partial \boldsymbol{f}'} = -\lambda_2(0)$. With this gradient information, the correction term $\boldsymbol{f}'_{\mathbf{o}}$ determined by the NFSV-DA can be automatically calculation using an optimization solver such as the Limited-memory Broyden-Fletcher-Goldfarb-Shanno (L-BFGS) algorithm (see [22] for the details of L-BFGS).

4. Evaluations to abilities of NFSV-DA in improving prediction skill of weather and climate

Numerical weather forecast and climate prediction are often contaminated by both initial errors and model errors; and the NFSV-DA here aims at offsetting the prediction errors caused by them and thus improving the prediction level. Then we ask: how well does the NFSV-DA perform in predictions of weather and climate? Actually, since the NFSV-DA including the original OFV and renewed OFV here was proposed, it has been applied to the studies of predictability associated with high-impact weather event tropical cyclone (TC) and climate event El Niño predictions. Next, we will summarize the results of these studies and evaluate the potential role of the NFSV-DA in improving numerical weather forecast and climate prediction.

4.1. El Niño predictability

El Niño is a famous phenomenon of interannual time scale in the tropical Pacific Ocean and has great global effects on weather and climate anomalies. El Niño predictions are always very important for disaster prevention and mitigation. There are mainly two flavors of El Niño: one has a warm sea surface temperature (SST) center in the eastern tropical Pacific Ocean and is often named EP-El Niño while the other possesses a warm SST center in the central Pacific Ocean and is entitled as CP-El Niño [1]. Due to different climate effects of two flavors of El Niño, it is very necessary to predict the types of El Niño [20]. Presently, types of El Niño can only be distinguished with a lead time of 1-4 months in hindcast experiments [17]. In realistic forecasts, the prediction skill of the types of El Niño is almost zero. Results have shown that initial errors of particular structure can cause large prediction error of EP-El Niño; especially, the spring predictability barrier (SPB), which causes the prediction skill of El Niño decreasing rapidly when predictions are made bestride spring and is often encountered by El Niño predictions, has been thought of as being resulted from the initial error effects [10,16,25,35]. For CP-El Niño events, Tian and Duan [33] demonstrated that they are more predictable than the EP-El Niño events without the effects of model errors, whereas in realistic forecasting, the EP-El Niño events usually present higher forecasting skill than the CP-El Niño events. Beyond doubt, it is model errors that cause such a contradiction. Furthermore, most of current models cannot simulate well the types of El Niño, which also reflects the effect of model error on simulation of types of El Niño. It is therefore inferred that, if predicting the types of El Niño, both initial errors and model errors are ought to be jointly considered. As mentioned earlier, the NFSV-DA deals with reduction of prediction error caused by initial and model errors, which exactly meets the need of prediction of types of El Niño. Now we just evaluate how well it performs in improving predictions of types of El Niño by retrospecting previous results.

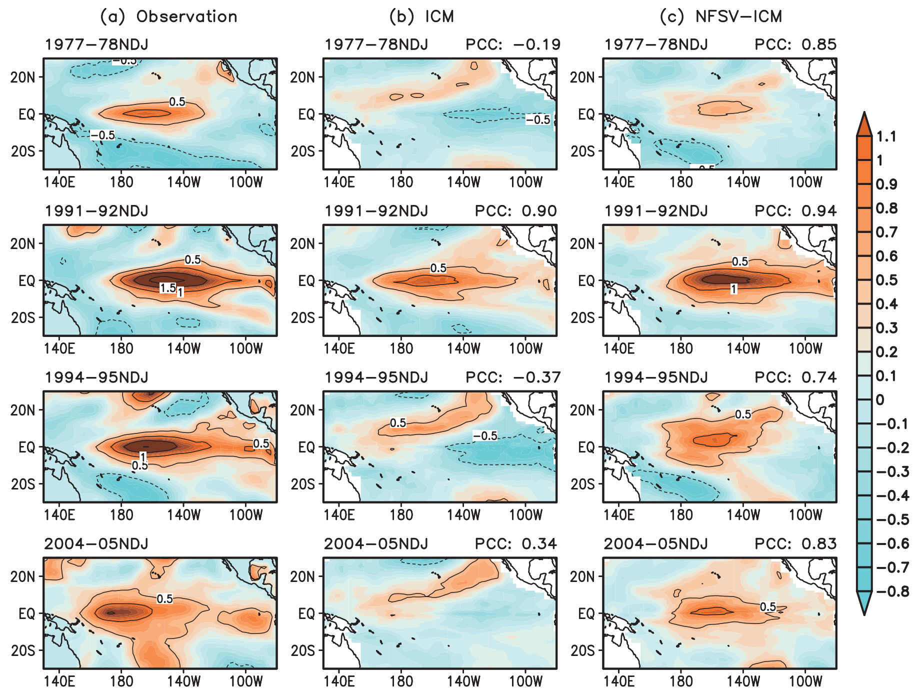

Figure 1. The winter SST patterns of CP-El Niño in the (a) observations, (b) ICM predictions and (c) NFSV-ICM predictions, where the lead time is six months. The PCC is the spatial correlation coefficient between the observation and prediction. The NFSV-ICM, compared with the ICM, reproduced successfully CP-El Niño events of concerned much well. This figure is from [32].

Tao and Duan [31] applied the NFSV-DA to an intermediate complex model (ICM; [36]) and established a new ENSO forecasting system: NFSV-ICM, which, due to the use of the NFSV-DA approach, considers the reduction of prediction errors caused by initial and model errors. When the NFSV-ICM was used to predict the El Niño events after the middle of 1970s, it can predict well the dominant SST anomaly modes of EP- and CP-El Niño events in their mature phases while the original ICM predicts CP-El Niño into either an EP-El Niño event or a cool event and fails to output CP-El Niño in predictions (see Figure 1); especially, the NFSV-ICM greatly weakened the effect of SPB phenomenon (see [31, 32]). If it is the question that how long the NFSV-ICM can predict which type of El Niño will occur, the results in Tao et al. [32] suggested that the NFSV-ICM can identify the types of El Niño at a lead time of at least 7 months. It is obvious that the ability of the NFSV-ICM identifying the types of El Niño in predictions is greatly superior to that of the lead times 1-4 months shown in previous study [17].

The NFSV-ICM has also been applied in the real-time prediction of El Niño events during recent five years. For these El Niño predictions, there are many models internationally that underwent severe challenging [2]. For example, most of the models failed to predict 2015/16 strong El Niño event with a 12-month lead time and then subsequent double La Nina variability during 2016-2018 [21]; for the 2019 CP-El Niño event, many models tended to predict it a strong EP-El Niño event at the beginning of the year; and for the ongoing 2021/22 La Nina event, a lot of models are experiencing another confusing. However, for these events the NFSV-ICM performed well in predicting their warm and cold phases and even their types (see Figure 2 for 2019 CP-El Niño prediction made by the NFSV-ICM), certainly highlighting the advantages of the NFSV-DA in improving climate predictions.

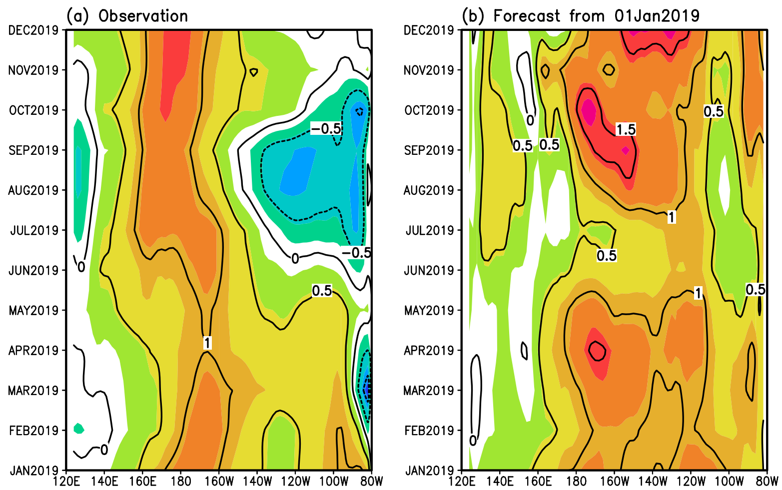

Figure 2. The observed SST anomalies from January 1st, 2019 to December 30th, 2019 and their predictions made by NFSV-ICM. (a) Observations and (b) predictions. The predictions captured the dominant mode of the observed SST anomalies, which exhibited a CP-El Niño event.

From above discussions, it is obvious that the NFSV-ICM has had a better performance in predicting and distinguishing the types of El Niño events. Of course, this is due to the fact that the NFSV-ICM offsets effect of both initial errors and model errors by the NFSV-DA. With this skill, it is expected that the NFSV-ICM can continue to keep better performance in the future predictions; even with the increasing of new observations, the NFSV-DA can show greater advantages in future predictions of ENSO.

4.2. TC intensity and rainfall

TCs are a kind of typical high-impact weather events, which are an intense circular storm phenomenon that originates over warm tropical oceans and is characterized by low atmospheric pressure, high winds, and heavy rain. TCs cause the most dramatic and damaging effects and then the forecasts of TCs are extremely important for disaster prevention and mitigation. TC track and intensity and accompanied rainfall are often concerned for TC forecasts. The forecasts of TC track have been greatly improved in recent 30 years despite there still exist non-negligible uncertainties [5, 13]; in contrast, the forecasting level of TC intensity is far behind that of the TC track, even the forecast of TC rainfall is much worse. Some studies emphasized effect of the errors occurring in intensity and structure of initial eddy on TC intensity forecasts while other studies thought that model errors play a much important role in yielding forecasting uncertainties of TC intensity [4, 15]. In any case, it is logical that TC intensity forecasts require to jointly consider initial errors and model errors, which certainly provides an opportunity to evaluate the role of the NFSV-DA in offsetting the error effects and improving TC forecasting level. In this section, we evaluate the usefulness of the NFSV-DA in neutralizing prediction errors caused by initial errors and model errors.

Qin et al. [29] first applied the NFSV approach of dealing with the most disturbing model error (i.e. solving the a maximization problem) to identify the optimally-growing tendency perturbations of nine TC cases using the Weather Research and Forecasting (WRF; http://www.wrf-model.org/) model. Then they concluded that these tendency perturbations result in the largest departure of the TC intensity measured by sea level pressure (SLP) from the reference simulations; especially, they emphasized the much strong sensitivity of potential temperature change, compared to that of moisture change, in causing this departure. Then Qin et al. [29] demonstrated that the forecast of the TC intensity with a 24-hour lead time is more sensitive to the change of the potential temperature than to that of the moisture; especially being sensitive to the changes of potential temperature in the lower and middle layers of the atmosphere around the center of the TCs. In view of this result, it can infer that the potential temperature change is one of sensitive meteorological factors and the area of the lower and middle layers of the atmosphere around the center of the TCs represents the sensitive area of TC intensity forecasts at the 24-hour lead time. As expected, when the NFSV-DA was applied to the tendency equation of potential temperature and an appropriate correction term was obtained to offset combined effect of initial errors and model errors, the forecasted minimum SLPs, i.e. the TC intensity, are much closer to the best-track data than the reference forecasts (Figure 3) (see [8, 29]). This reflects the strong sensitivity of the TC intensity to the change of potential temperature, also sheds light on that NFSV sensitivity and NFSV-DA are mutually supported dynamically.

For TC rainfalls, they were shown to be more sensitive to the moisture change, and then the NFSV-DA was applied to the moisture tendency, finally improving the TC rainfall forecasting level (see [29]). As an example, for the TC case Dujuan, the rainfall is mainly concentrated at -6 h (i.e. the 6 hours before initial time of forecasts), then decreases rapidly after 0 h (i.e. the initial time), and finally becomes zero at 6 h in the reference forecast (see Figure 4). However, when the NFSV-DA was applied to the tendency of the moisture tendency equation, the rainfall appears at 6 h, which coincides with the fact. All these indicate that the correction of moisture change contributes to the improvement of TC rainfall forecasts much more, which reflects the strong sensitivity of the TC rainfall on the moisture change revealed by the NFSV. Simultaneously, this indicates that the NFSV-DA can effectively reduce effect of prediction uncertainties enhanced by the moisture change sensitivity, eventually showing its usefulness in improving TC intensity and rainfall forecast.

5. Summary and discussion

The NFSV approach for dealing with the most sensitive model error and the OFV approach for offsetting model error effects were reviewed. Relating OFV to NFSV,

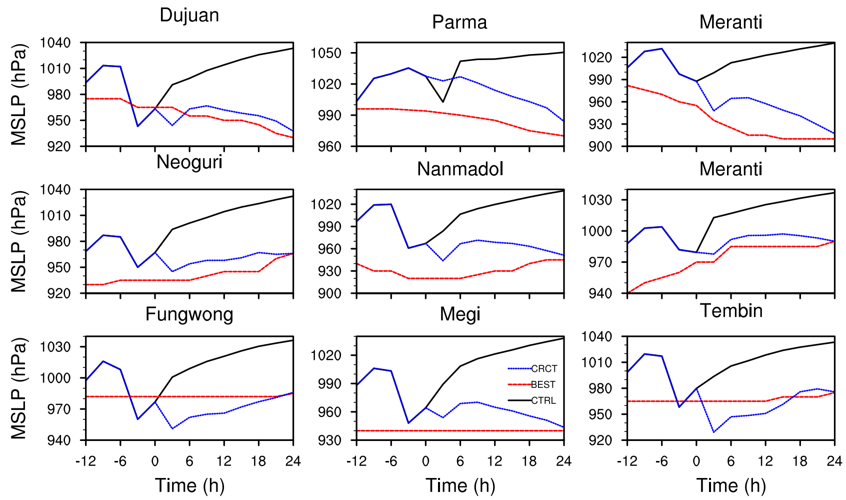

Figure 3. The intensity forecasts of nine TCs the NFSV-DA. Red lines represent the observed TC intensities measured by the minimum SLP, black lines are for the reference forecasts, and the blue lines denote the forecasts made by the NSFV-tendency assimilation, which, compared to the reference forecasts, are much close to the observation. This figure is from Duan and Qin [8].

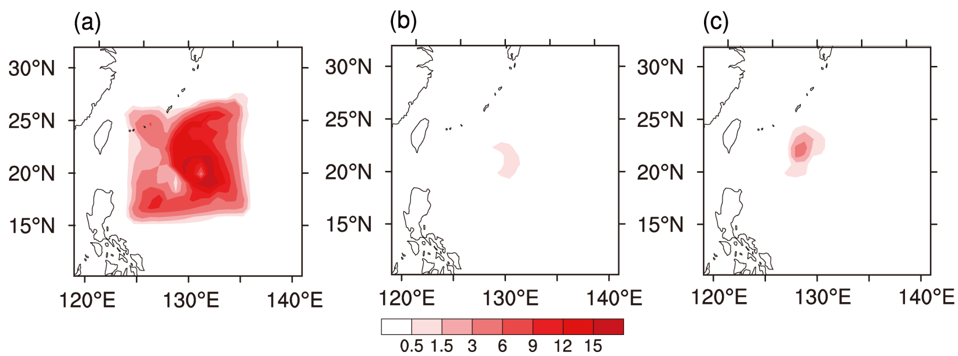

Figure 4. TC rainfall (> 0.5 mm; red color) at −6 h (a) and 0 h (b) in reference forecast, and at 6 h in the forecast made by the NFSV-DA (c) for the TC case Dujuan, respectively. The forecast made by the NFSV-DA presented the rainfall at 6 h, which did not appear in reference. This figure is from Qin et al. [29].

we updated the OFV to the "NFSV-DA" approach for neutralizing combined effect of model errors and initial errors. The gradient of the cost function with respect to tendency perturbation was derived to solve the large scale of optimization problem of the NFSV-DA. Thus, a novel approach of data assimilation is prepared for numerical weather forecast and climate prediction.

Applications to high-impact weather and climate event forecasts were retrospected to evaluate the potential role of the NFSV-DA in improving forecasting levels. Specifically, for both El Niño prediction and TC forecast, the NFSV-DA can help improve greatly the prediction levels of El Niño diversity and TC intensity and rainfall, especially making a breakthrough in overcoming SPB effect and reproducing TC rainfall in predictions. Therefore, the NFSV-DA has potential for becoming a useful assimilation approach for offsetting combined effect of model errors and initial errors and improving weather and climate prediction skill.

Despite the NFSV-DA has achieved successful applications in prediction of El Niño and TCs, it remains unknown whether or not the NFSV-DA is still useful when it is used to the forecasts of other weather and climate events. Therefore, more weather and climate phenomena should be investigated to explore the robustness of the usefulness of the NFSV-DA in improving prediction level. For the calculation of the NFSV-DA, although the adjoint-related gradient was derived to enable itself applicable for solving predictability problem of large scale, it is still time consuming and limits the efficiency of real-time weather forecast. Furthermore, it is not all numerical models that possess an adjoint; especially, developing the adjoint of a model is cumbersome and time-consuming, which greatly limits the widespread applications of the NFSV-DA. It is therefore that a much efficient algorithm should be developed to calculate the NFSV-DA, especially avoidance of the use of adjoint models. In any case, there are still works to consummate the NFSV-DA approach. And it is expected that the NFSV-DA will be much useful in improving weather and climate predictions.

Acknowledgements

This work was jointly sponsored the National Nature Scientific Foundation of China (Nos. 41525017, 41930971).

References

[1] K. Ashok, S. Behera, S. Rao et al., *El Niño Modoki and its possible teleconnection*, J. Geophys. Res. Ocean, 2007, 112, C11007.

[2] A. Barnston, M. Tippett, M. L'Heureux et al., *Skill of real-time seasonal ENSO model predictions during 2002-11: Is our capability increasing?*, Bulletin of the American Meteorological Society, 2012, 93(5), 48.

[3] P. Bauer, A. Thorpe and G. Brunet, *The quiet revolution of numerical weather prediction*, Nature, 2015, 525, 47–55.

[4] K. Bhatia, D. Nolan, A. Schumacher and M. DeMaria, *Improving tropical cyclone intensity forecasts with PRIME*, Weather and Forecasting, 2017, 32, 1353–1377.

[5] M. Demaria, C. Sampson, J. Knaff and coauthors., *Is tropical cyclone intensity guidance improving?*, Bull. Amer. Meteorol. Soc., 2014, 95, 387–398.

[6] W. Duan, C. Huang and H. Xu, *Nonlinearity modulating intensities and spatial structures of Central Pacific- and Eastern Pacific-El Niño events*, Adv. Atmos. Sci., 2017, 34, 737–756.

[7] W. Duan, X. Li and B. Tian, *Towards optimal observational array for dealing with challenges of El Niño-Southern Oscillation predictions due to diversities of El Niño*, Clim. Dynam., 2018, 51, 3351–3368.

[8] W. Duan and X. Qin, *Nonlinear optimal perturbations and its applications to the studies of tropical cyclone target observations and associated with field campaigns (in Chinese)*, Advances in Earth Sciences, 2022, Accepted.

[9] W. Duan, B. Tian, and H. Xu, *Simulations of two types of El Niño events by an optimal forcing vector approach*, Clim. Dynam., 2014, 43, 1677–1692.

[10] W. Duan and C. Wei, *The spring predictability barrier for El Niño events and its possible mechanism results from a fully coupled model*, Inter. J. Climatology, 2012, 33, 1280–1292.

[11] W. Duan and P. Zhao, *Revealing the most disturbing tendency error of Zebiak-Cane model associated with El Niño predictions by nonlinear forcing singular vector approach*, Clim. Dynam., 2014, 44, 2351–2367.

[12] W. Duan and F. Zhou, *Non-linear forcing singular vector of a two-dimensional quasi-geostrophic model*, Tellus A, 2013, 65, 18452.

[13] K. Emanuel and F. Zhang, *On the predictability and error sources of tropical cyclone intensity forecasts*, J. Atmos. Sci., 2016, 73, 3739–3747.

[14] F. Feng and W. Duan, *The role of constant optimal forcing in correcting forecast model*, Sciences in China (D), 2013, 56, 434–443.

[15] B. Green and F. Zhang, *Impacts of air-sea flux parameterizations on the intensity and structure of tropical cyclones*, Mon. Wea. Rev., 2013, 141, 2303–2324.

[16] J. Hu and W. Duan, *Relationship between optimal precursory disturbances and optimally growing initial errors associated with ENSO events : Implications to target observations for ENSO prediction*, J. Geophys. Res. Ocean, 2016, 121, 011386.

[17] H. Jeong, D. Lee, K. Ashok and coauthors, *Assessment of the APCC coupled MME suite in predicting the distinctive climate impacts of two favors of ENSO during boreal winter*, Clim. Dynam., 2012, 39, 475–493.

[18] E. Kalney, *Atmospheric Modeling, Data Assimilation, and Predictability*, Cambridge University Press, Cambridge, UK, 2003.

[19] B. Kirtman, S. Power, J. Adedoyin et al., *Climate Change 2013: The Physical Science Basis. Contribution of Working Group I to the Fifth Assessment Report of the Intergovernmental Panel on Climate Change*, Cambridge University Press, Cambridge, UK, 2013.

[20] R. Lee, C. Tam, S. Sohn and J. Ahn, *Predictability of two types of El Niño and their climate impacts in boreal spring to summer in coupled models*, Clim. Dynam., 2018, 51, 4555–4571.

[21] M. L'Heureux, K. Takahashi, A. Watkins et al., *Observing and predicting the 2015-16 El Nino*, Bulletin of the American Meteorological Society, 2017, 98(7), 1363–1382.

[22] C. Liu and J. Nocedal, *On the limited memory method for large scale optimization*, Mathematical Programming B, 1989, 45, 503–528.

[23] E. Lorenz, *Predictability of weather and climate*, Cambridge University Press, Cambridge, UK, 1996.

[24] E. Lorenz and K. Emanuel, *Optimal sites for supplementary weather observations: Simulation with a small model*, J. Atmos. Sci., 1998, 55, 399–414.

[25] A. Moore and R. Kleeman, *The dynamics of error growth and predictability in a coupled model of ENSO*, Q. J. R. Meteorol. Soc., 1996, 122, 1405–1446.

[26] M. Mu, W. Duan, D. Chen et al., *Target observations for improving initialization of high-impact ocean-atmospheric environmental events forecasting*, Natl. Sci. Rev., 2015, 2, 226–236.

[27] M. Mu, W. Duan and J. Chou, *Recent advances in predictability studies in China (1999–2002)*, Adv. Atmos. Sci., 2004, 21, 437–443.

[28] T. Palmer, *Predicting uncertainty in forecasts of weather and climate*, Rep. Prog. Phys., 2000, 63, 71–116.

[29] X. Qin, W. Duan and H. Xu, *Sensitivity on tendency perturbations of tropical cyclone short-range intensity forecasts generated by WRF*, Adv. Atmos. Sci., 2020, 37, 291–306.

[30] C. Snyder, *Summary of an informal workshop on adaptive observations and FASTEX*, Bull. Amer. Meteor. Soc., 1996, 77, 953–961.

[31] L. Tao and W. Duan, *Using a nonlinear forcing singular vector approach to reduce model error effects in ENSO forecasting*, Weather and Forecasting, 2019, 34, 1321–1342.

[32] L. Tao, W. Duan and S. Vannitsem, *Improving forecasts of El Niño diversity: a nonlinear forcing singular vector approach*, Clim. Dynam., 2020, 55, 739–754.

[33] B. Tian and W. Duan, *Comparison of constant and time-variant optimal forcing approaches in El Niño simulations by using the Zebiak-Cane model*, Adv. Atmos. Sci., 2016, 33, 685–694.

[34] J. Wang, J. Chen, J. Du and coauthors, *Sensitivity of ensemble forecast verification to model bias*, Mon. Wea. Rev., 2018, 146, 781–796.

[35] Y. Yu, W. Duan, H. Xu and M. My, *Dynamics of nonlinear error growth and season-dependent predictability of el niño events in the zebiak-cane model*, Q. J. R. Meteorol. Soc., 2009, 135, 2146–2160.

[36] R. Zhang, S. Zebiak, R. Kleeman and N. Keenlyside, *A new intermediate coupled model for El Niño simulation and prediction*, Geophys. Res. Lett., 2003, 30, 018010.